BIOCHEMISTRY
including biophysical chemistry & molecular biology

ARTICLE

pubs.acs.org/biochemistry

The Membrane Interface Dictates Different Anchor Roles for "Inner Pair" and "Outer Pair" Tryptophan Indole Rings in Gramicidin A Channels

Hong Gu,[†] Kevin Lum,[‡] Jung H. Kim,[‡] Denise V. Greathouse,[†] Olaf S. Andersen,[*,‡] and Roger E. Koeppe, II[*,†]

[†]Department of Chemistry and Biochemistry, University of Arkansas, Fayetteville, Arkansas 72701, United States

[‡]Department of Physiology and Biophysics, Weill Cornell Medical College, New York, New York 10065, United States

ABSTRACT: We investigated the effects of substituting two of the four tryptophans (the "inner pair" Trp^{9} and Trp^{11} or the "outer pair" Trp^{13} and Trp^{15}) in gramicidin A (gA) channels. The conformational preferences of the doubly substituted gA analogues were assessed using circular dichroism spectroscopy and size-exclusion chromatography, which show that the inner tryptophans 9 and 11 are critical for the gA's conformational preference in lipid bilayer membranes. [$Phe^{13,15}$]gA largely retains the single-stranded helical channel structure, whereas [$Phe^{9,11}$]gA exists primarily as double-stranded conformers. Within this context, the ^{2}H NMR spectra from labeled tryptophans were used to examine the changes in average indole ring orientations, induced by the Phe substitutions and by the shift in conformational preference. Using a method for deuterium labeling of already synthesized gAs, we introduced deuterium selectively onto positions C2 and C5 of the remaining tryptophan indole rings in the substituted gA analogues for solid-state ^{2}H NMR spectroscopy. The (least possible) changes in orientation and overall motion of each indole ring were estimated from the experimental spectra. Regardless of the mixture of backbone folds, the indole ring orientations observed in the analogues are similar to those found previously for gA channels. Both Phe-substituted analogues form single-stranded channels, as judged from the formation of heterodimeric channels with the native gA. [$Phe^{13,15}$]gA channels have Na^{+} currents that are ~50% and lifetimes that are ~80% of those of native gA channels. The double-stranded conformer(s) of [$Phe^{9,11}$]gA do not form detectable channels. The minor single-stranded population of [$Phe^{9,11}$]gA forms channels with Na^{+} currents that are ~25% and single-channel lifetimes that are ~300% of those of native gA channels. Our results suggest that Trp^{9} and Trp^{11}, when "reaching" for the interface, tend to drive both monomer folding (to "open" a channel) and dimer dissociation (to "close" a channel). Furthermore, the dipoles of Trp^{9} and Trp^{11} are relatively more important for the single-channel conductance than are the dipoles of Trp^{13} and Trp^{15}.

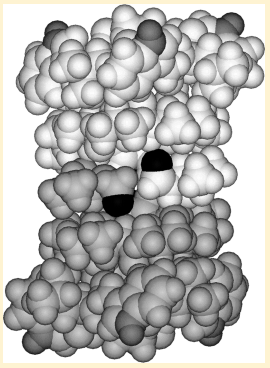

The physicochemical principles underlying membrane protein structure and function remain a challenge because of the nature of biological membranes, being thin and heterogeneous in chemical composition, yet it is critical to understand how the amino acid sequence determines both the structural preference and function of membrane proteins. In this context, the gramicidin A (gA) channels play an important role because, though relatively small in size, they have very well-defined properties. They thus are useful tools for studying the principles that govern membrane protein structure and function.

An important feature of the gA channels is the presence of four tryptophan residues in each subunit. The subunit sequence is formyl-VGALAVVVW^{9}LW^{11}LW^{13}LW^{15}-ethanolamide (D-residues underlined). In gA channels, tryptophan has several roles. The eight Trp side chains orient the dimeric channel.[1] They stabilize the single-stranded dimeric conformation,[2−6] and they promote the transport of cations through the channel through favorable ion−dipole interactions.[7−12] These observations suggest that tryptophan may make important contributions to the folding and function of membrane proteins.

The unique side chain characteristics of Trp are believed to be important to membrane proteins in general. Trp is a large aromatic, amphiphilic amino acid with a dipole moment of ≈2 D along the C5 → N1 axis.[13] Substitutions of Trp with the more hydrophobic Phe have revealed important information about gA channels. For example, there is an ~2-fold decrease in the conductance of the channels formed by [Phe^{11}]gA, a natural product in the host organism *Bacillus brevis*.[14,15] Early studies showed that substitution of one, two (at positions 9 and 15 only), three, or four Trp residues with Phe significantly decreases the gA channel conductance[7,14,16] and that this effect is not evenly distributed.[7]

Recent evidence, based on analogues with 1-methylation of the indole ring nitrogen,[17] has suggested that the influence of Trp^{9} and Trp^{11} (designated the "inner pair" Trps) on gramicidin structure and function is rather different from the influence of Trp^{13} and Trp^{15} (the "outer pair"). The detailed effects induced by the pairwise "double" Trp → Phe substitutions (inner pair of Phe^{9} and Phe^{11} or outer pair of Phe^{13} and Phe^{15}) have not been investigated, however.

Recently, we developed a method for deuterium labeling of Trp indole ring positions 2 and 5 in intact gramicidins.[18] Here we

Received: January 26, 2011
Revised: April 29, 2011
Published: May 03, 2011

apply the labeling method to the two remaining Trps in each of the doubly Phe-substituted gramicidins. The method allows us to report the consequences for the average ring orientations of the remaining tryptophans when a pair of Trps in a gramicidin subunit (inner pair or outer pair) is replaced with two phenylalanines. We also compare the properties of the channels formed by the inner and outer doubly substituted analogues with results from other Phe substitutions using single-channel electrophysiology,[7] complemented by structural studies using CD spectroscopy, size-exclusion chromatography, and solid-state deuterium nuclear magnetic resonance (NMR) spectroscopy. (The functional characterization of the four simultaneous Trp → Phe substitutions, in [Phe^{9,11,13,15}]gA, has been reported previously.[3,4,19])

Our results indicate that [Phe^{13,15}]gA folds predominantly into the single-stranded (SS) channel structure and that [Phe^{9,11}]gA folds predominantly into one of several possible (inert, or nonconducting) double-stranded (DS) structures, in agreement with an earlier characterization by SEC.[20] Regardless of the folding preference, the Trp indole ring orientations change very little in [Phe^{9,11}]gA or [Phe^{13,15}]gA. The single-channel results show that the SS [Phe^{9,11}]gA channels have increased lifetimes, whereas the [Phe^{13,15}]gA channels have decreased lifetimes, indicating that the analogues' conformational preference is not a determinant of the SS channel lifetimes. Both pairs of Phe substitutions reduce the single-channel conductance, but the decrease is more pronounced when the inner pair (Trp^9 and Trp^{11}) are removed to yield the [Phe^{9,11}]gA channels.

MATERIALS AND METHODS

Materials. Fmoc-Trp Wang resin and unlabeled Fmoc-protected amino acids were purchased from Advanced Chem Tech (Louisville, KY) and NovaBiochem (San Diego, CA). DMPC and DPhPC were from Avanti Polar Lipids (Alabaster, AL). Deuterated TFA (CF_3COOD), deuterium-depleted water, and D_2O were purchased from Cambridge Isotope Laboratories (Andover, MA). Methanol was from Burdick&Jackson (Muskegon, MI), and tetrahydrofuran from Waters, Inc. (Milford, MA). Regular filtered water was doubly deionized Milli-Q water.

Peptide Synthesis. The Phe gramicidin analogues were synthesized on an Applied Biosystems 433A synthesizer using standard Fmoc chemistry[21] and Trp Wang resin (Advanced Chem Tech). After the last synthesis step, peptides were finished by formylation. Following addition of 2.5 mL of DMF containing 80 mg of *p*-nitrophenyl formate and 0.01 mL of *N*-methylmorpholine, the resin was stirred at 4 °C overnight. The resin was washed with DMF, and the peptide was cleaved from the resin with 20% ethanolamine in DMF at 25 °C for 48 h.[21] The peptide sequences are formyl-V^1-G-A-L-A-V-V^7-V-W-L-W-L-W-L-W^{15}-ethanolamine (D-residues underlined), but with Phe (F) substitution instead of Trp (W) at positions 9 and 11 or positions 13 and 15. The identity and purity of the gramicidin analogue were confirmed by electrospray ionization MS and reversed-phase HPLC (Zorbax SB80, 4.6 mm × 50 mm column of 3.5 μm octylsilica, from MacMod analytical, Chadds Ford, PA).

Isotope Exchange. *Exchange of ^{2}H into the Indole Ring in Gramicidin Analogues.* Deuterium was introduced on indole rings in existing peptides (postsynthesis). In detail, 20 mg of the gramicidin analogue was weighed into a 4 mL glass vial equipped with a Teflon cap. Cold CF_3COOD (0.5 mL, precooled on ice) was added to the vial with the gramicidin (all on ice). Because darkness is essential for preventing damage to the indole ring, the vial was covered with aluminum foil as quickly as possible. The solution was shaken in a cold room (4 °C) for 20 min. (Longer reaction times or higher temperatures cause damage to the peptide.[22]) While the reaction is underway, it is essential to have 5 mL of cold water ready in a centrifuge tube (polystyrene, 20 mL). Following the reaction, the TFA/gramicidin solution was transferred into the precooled, water-containing tube to precipitate the deuterated gramicidin. After centrifugation in the cold (6000 rpm at 4 °C), the supernatant water was decanted. The deuterated gramicidin was washed three more times with water (using deuterium-depleted water for the last wash), followed by centrifugation. The resulting pellet was dried under vacuum (10^{-3} mmHg). Finally, to remove final traces of residual TFA, the deuterated gramicidin was dissolved in 1 mL of methanol and dried by vacuum centrifugation, twice.

Solid-State ^{2}H NMR Spectroscopy. *Oriented Sample Preparation.* Aligned gramicidin/lipid samples were prepared using the procedure described by van der Wel et al.[23] Each sample consisted of 4 μmol of gramicidin and 80 μmol of DMPC to maintain a gramicidin:lipid molar ratio of 1:20. Gramicidin/lipid samples in a chloroform/methanol mixture were distributed evenly onto approximately 40 glass slides (4.8 mm × 23 mm × 0.07 mm). Samples were dried first under a stream of N_2 and then under vacuum and then hydrated using deuterium-depleted water to achieve 45% (w/w) overall hydration, which ensures fully hydrated bilayers.[24] Before the NMR measurements, the samples were allowed to equilibrate at 40 °C for at least 72 h to secure optimal alignment.

NMR Measurements. To investigate the tryptophan conformations,[25,26] ^{2}H NMR spectra were recorded with the lipid bilayer normal aligned either parallel to the magnetic field ($\beta = 0°$) or perpendicular ($\beta = 90°$), using a Bruker AMX2 300 spectrometer, operating at 46 MHz for ^{2}H.[27] Measurements were taken at 50 °C, to maintain the lipids in the liquid-crystalline phase[28] and to optimize the detection of ^{2}H resonances (see also ref 26). The ^{2}H measurements involved 3−5 million acquisitions and were taken using a quadrupolar echo pulse sequence[29] with an echo delay of 125 μs, a 90° pulse duration of 3.3 μs, and a 60 ms interpulse time. A line broadening of 400 Hz was applied to the ^{2}H spectra. Phosphorus (^{31}P) NMR experiments were performed to check the alignment of the lipid bilayers.[23]

Data Analysis. ^{2}H NMR spectra have been used to examine the average orientations of Trp indole rings in gA channels.[5,11,25] Each deuterium nucleus produces two symmetric peaks, separated by their quadrupolar splitting. The quadrupolar splittings can be converted to orientation angles for the individual C−D bonds on the indole ring:

$$\Delta\nu_q = \frac{3}{2}S_{zz}\left(\frac{e^2qQ}{h}\right)\left[\frac{1}{2}(3\cos^2\theta - 1)\right]\left[\frac{1}{2}(3\cos^2\beta - 1)\right]$$

In this equation, e^2qQ/h is the quadrupolar coupling constant (QCC), which for deuterons on aromatic rings has a measured static value of ∼180 kHz.[30] The "effective" quadrupolar coupling constant may be reduced by molecular motion,[31] which is estimated by a principal order parameter S_{zz} between 0 and 1.[25] Angle θ is the angle between a particular C−D bond and the membrane normal; angle β is the angle between the membrane normal and the magnetic field, either 0° or 90°. For gA channels, the helix axis also is aligned with the membrane normal.[25,32] Assignments of quadrupolar splittings to the C2−D and C5−D indole ring bonds were based upon the relative peak intensities and the known position-dependent kinetics for the indole ring

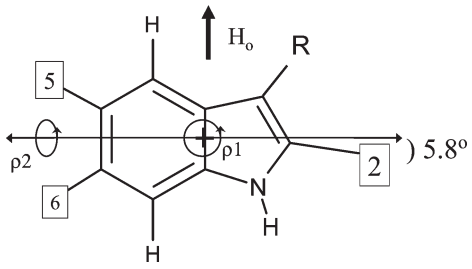

Figure 1. Indole ring geometry and rotational degrees of freedom, ρ_1 and ρ_2, for orienting the ring with respect to an external magnetic field. Ring positions 2, 5, and possibly 6 (numbered) become labeled, to different extents, by the $^1H-^2H$ exchange reaction described in Methods. The C2−H bond makes an angle of 5.8° with an axis that bisects the six-membered ring.[25] Modified from ref 32.

isotope exchange.[25] Changes in indole ring average orientation and dynamics were estimated by calculating the backbone-independent ring orientation angles ρ_1 and ρ_2 (Figure 1), as the "effective" quadrupolar coupling constant (QCC × S_{zz}) was searched, as described previously.[25] In this method, the root-mean-square deviation (rmsd) between observed and calculated quadrupolar splittings is calculated for all possible values of ρ_1 and ρ_2 for a particular S_{zz}; the reported ρ_1 and ρ_2 values for each S_{zz} are those for which the rmsd was smallest.

Circular Dichroism Spectroscopy and Size-Exclusion Chromatography. Samples having a gramicidin:lipid ratio of 1:50 were prepared using salt-free DMPC as described in ref 33. UV absorbance at 280 nm, where ε = 5210 Trp^{-1} M^{-1} cm^{-1},[34] was used to determined the final gramicidin concentration in each sample. CD spectra were recorded at room temperature using a Jasco J710 CD spectrometer with a 0.1 cm path length cell, a 1.0 nm bandwidth, a 0.2 nm step resolution, and a 50 nm/min scan speed. Each spectrum is an average of six scans.

The fractions of double-stranded (DS) and single-stranded (SS) conformers of each gA analogue were estimated using size-exclusion chromatography (SEC) in lipid suspensions.[17,20,35] The gramicidin/lipid dispersions were injected into an Ultrastyrogel 1000 Å column [7 μm, 7.8 mm × 300 mm; mobile phase being 100% tetrahydrofuran at a rate of 1.0 mL/min (Waters, Inc.)], and the elution times for DS and SS conformers were recorded.

Single-Channel Measurements. Planar bilayers were formed from *n*-decane solutions (2.5%, w/v) of DPhPC, across a hole (~1.6 mm diameter) in a Teflon partition that separates two 1.0 M NaCl aqueous solutions at pH 7.0. Single-channel measurements were taken at 25 ± 1 °C using the bilayer punch method,[36] using pipettes with a tip diameter of ~30 μm and a Dagan 3900 patch clamp amplifier (Dagan Corp., Minneapolis, MN). The applied potential was ±200 mV, with the front (or *cis*) chamber being the electrical reference (at 0 mV) and the bilayer punch in the rear (or *trans*) chamber.

The gA analogues were added from stock dilutions, made up in either ethanol or DMSO, to the electrolyte solution on both sides of the bilayer. The final concentrations were ~2 pM for gA and [$Phe^{13,15}$]gA and 20 pM for [$Phe^{9,11}$]gA. The aqueous solution was stirred for 60 s after peptide addition, and the final ethanol or DMSO concentration was less than 0.25%, a concentration that has no effect on channel properties.[37] The current signal was filtered at 2 kHz, digitized at 20 kHz, and digitally filtered at 500 Hz. Single-channel current transitions were detected online and analyzed as described previously.[38−40] The transition amplitudes and lifetime distributions are based on independent measurements at each polarity. The lifetime histograms were transformed into survivor distributions, with average channel lifetimes (τ) determined by fitting a single-exponential distribution [$N(t)/N(0) = \exp(-t/\tau)$, where $N(t)$ denotes the number of channels with a lifetime longer than time t] to each histogram.[39]

In the heterodimer formation experiments, we used two different protocols. Most experiments were conducted with symmetric addition of both gramicidins to both sides of the bilayer, at the same concentrations that were used when characterizing the individual compounds. The solutions were stirred (for 60 s), and the channel activity was recorded and analyzed as described above. In each experiment, we isolated 3−10 "small" membranes using the bilayer punch; the distribution of single-channel current transition amplitudes was similar among the recordings conducted with the different small membranes. In the experiments where we probed the orientation of the heterodimeric channels with respect to the applied potential, we added the amino acid-substituted gA analogue to only the *cis* compartment and gA to only the *trans* compartment (again stirring for 60 s after the gramicidins had been added) and recorded the single-channel activity at 200 and −200 mV.

RESULTS

Conformational Preference. Because successive Trp → Phe (or Trp → 1-Me-Trp) substitutions increase the propensity for folding into DS conformations as opposed to the SS channel conformation,[17,20] even in lipid membrane environments, we tested the conformational preferences following Phe substitutions of the inner pair (Trp^9 and Trp^{11}) or the outer pair (Trp^{13} and Trp^{15}). The CD spectrum of [$Phe^{13,15}$]gA (Figure 2D) shows positive ellipticity between 210 and 240 nm, but with an intensity lower than that observed for native gA (Figure 2E), suggestive of a mixture of SS and DS conformations. By contrast, the CD spectrum of [$Phe^{9,11}$]gA (Figure 2C) shows negative ellipticity between 210 and 240 nm, suggestive of predominantly DS conformations.[33] These findings were confirmed by SE chromatography; in agreement with an earlier report,[20] [$Phe^{9,11}$]gA (Figure 2A) is ~75% DS (as peak 1 dominates in the SE chromatograms) whereas [$Phe^{13,15}$]gA (Figure 2B) is ~75% SS (as peak 2 predominates in the SE chromatograms). (The later small peaks in the chromatograms are due to changes in the refractive index upon elution of the lipids.) On the basis of these comparisons, we deduce that the inner tryptophans 9 and 11 are of major importance for maintaining the cation-conducting, membrane-spanning SS channel conformation. Even though the [$Phe^{9,11}$]gA population is ~75% DS, it is the minor SS population that comprises the cation-conducting channels (see below).

Single-Channel Properties. Each of the doubly substituted Phe analogues forms channels in bilayer membranes of DPhPC (Figures 3 and 4). gA and [$Phe^{13,15}$]gA have comparable channel forming potencies, meaning that we needed to add similar amounts to observe similar channel appearance rates; [$Phe^{9,11}$]gA had lower channel forming potency, as we needed to add 10-fold more of this analogue to observe the same channel appearance rates, suggesting that the [$Phe^{9,11}$]gA channels are formed by a minor conformer (generally consistent with the SEC results). Compared to those of native gA channels, the single-channel currents carried by Na^+ are reduced by ~50% when the

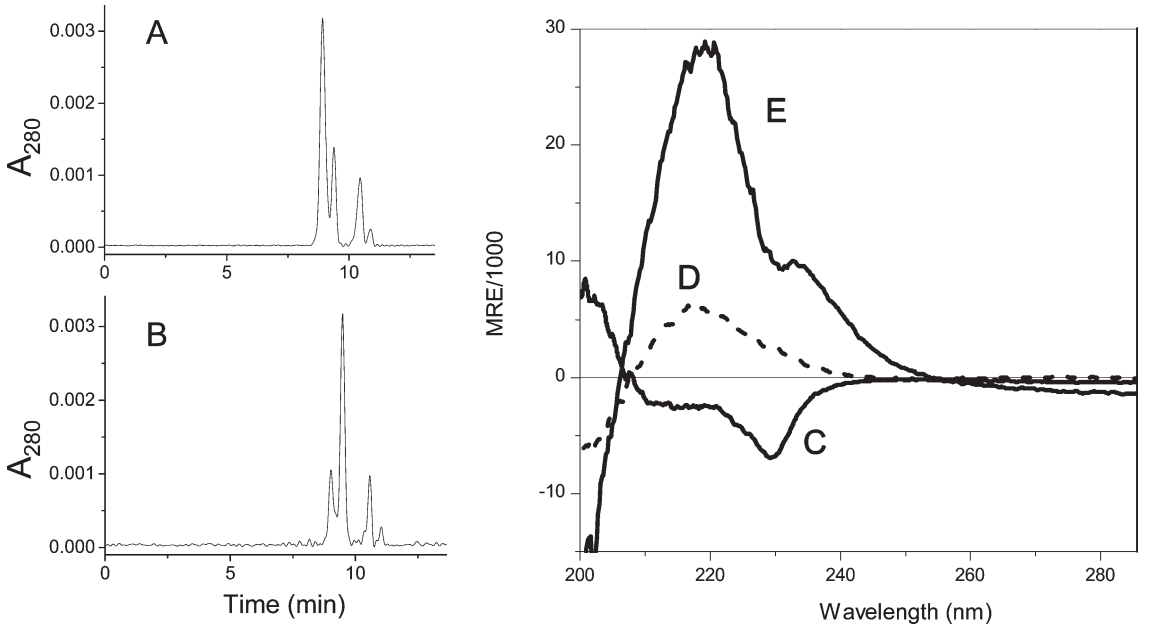

Figure 2. Conformational analysis of the gA analogues using SEC analysis and CD spectroscopy. (A and B) SEC chromatograms indicate a preference for double-stranded conformers (~75%) for [Phe^{9,11}]gA (A), compared to ~75% single-stranded conformer for [Phe^{13,15}]gA (B). The first two peaks, eluting at ~9.0 and ~9.5 min represent the DS and SS conformers, respectively (peaks eluting later than 10 min represent changes in the refractive index upon elution of lipids). (C–E) CD spectra of (C) [Phe^{9,11}]gA, (D) [Phe^{13,15}]gA, and (E) native gA. DMPC, 1:50 (gramicidin:lipid molar ratio), 25 °C.

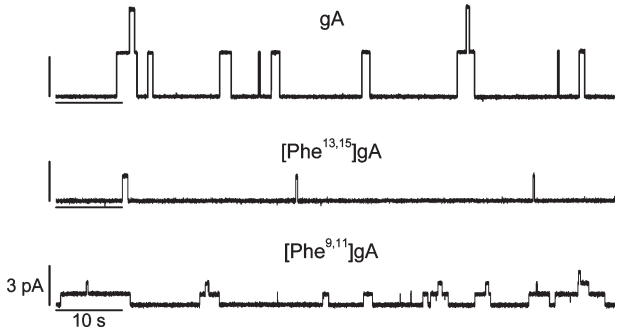

Figure 3. Single-channel current traces for channels formed by the native gA and the sequence-substituted [Phe^{13,15}]gA and [Phe^{9,11}]gA analogues. DPhPC, 1 M NaCl, 200 mV, 25 °C. The labels on the bottom calibration bars apply also to the calibration bars in the top two traces.

outer tryptophans are replaced ([Phe^{13,15}]gA) and by ~75% when the inner tryptophans are replaced ([Phe^{9,11}]gA) (Table 1).

Both gA and each of the analogues form channels with a single predominant current transition amplitude. The single-channel current transitions observed with [Phe^{9,11}]gA as well as [Phe^{13,15}]gA have a narrow current distribution (Figure 4A) typical of a single conducting conformation (functional conformer), and the single-channel lifetime distributions are described by single-exponential distributions (Figure 4B). The [Phe^{9,11}]gA single-channel lifetime is longer (Figure 4B) than that of native gA channels and comparable to that of [Phe^{9}]gA channels[7] (see also Table 1). We therefore deduce that the conducting [Phe^{9,11}]gA conformer is the minor SS conformer, not the major DS conformer, observed in the CD and SEC experiments (Figure 2). Likewise, the conducting conformer of [Phe^{13,15}]gA also is SS, with a single-channel lifetime that is slightly shorter than that of native gA and [Phe^{9,11}]gA channels (Figure 4B). Results for our doubly substituted Trp → Phe gA analogues are listed together with results for other analogues (from ref 7) in Table 1. Our assignment of the conformation of the conducting channels is confirmed in heterodimer experiments (see below). For each of the doubly substituted Phe gA analogues, the (presumably inert) DS conformers could not be observed by single-channel recording methods. The trends in the single-channel lifetimes indicate that having Trps at positions 9 and 11 will tend to decrease the lifetime, whereas having Trps at positions 13 and 15 has little effect on the single-channel lifetime (relative to having Phe at these positions).

Deuterium NMR Spectra. The deuterium isotope exchange method allowed us to estimate the Trp indole ring orientations using ^{2}H NMR spectroscopy. In Figure 5, we show the ^{2}H NMR spectra for isotope-exchanged samples of [Phe^{13,15}]gA and [Phe^{9,11}]gA in oriented DMPC bilayers. The taller two pairs of peaks in each spectrum represent signals from the fast-exchanging C2 deuterons[25] of the two remaining Trp rings in each gramicidin analogue. Each particular ring C2 assignment was deduced by assuming that the relative order of splittings would not change from the known assignments in gA.[25] Additional pairs of medium-intensity peaks represent signals from the respective C5 deuterons, which display weaker isotope enrichment because of slower exchange with deuterium during the sample preparation. The quadrupolar splittings and assignments for the major pairs of peaks are summarized in Table 2. For comparison, the quadrupolar splittings for the corresponding deuterons in native gA are also listed. The resonances from the C5 deuterons of Trp^{13} and Trp^{15} in native gA both exhibit a quadrupolar splitting of 205 kHz; the corresponding resonances in [Phe^{9,11}]gA are both near 211 kHz (Table 2).

The minor peaks in Figure 5 can be attributed to contributions from the significant amounts (~25%) of minor conformers, as well as small amounts of ^{2}H exchange at the C6 ring positions.[25] The presence of the minor peaks nevertheless does not interfere with

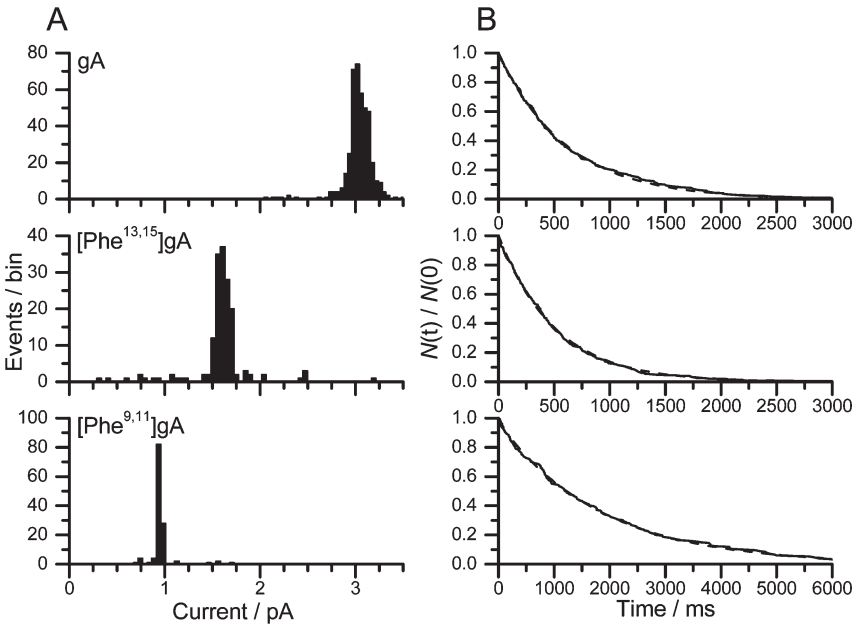

Figure 4. Single-channel amplitude and lifetime distributions for channels formed by the native gA and the sequence-substituted [Phe^{13,15}]gA and [Phe^{9,11}]gA analogues. (A) Amplitude histograms for gA channels, [Phe^{13,15}]gA channels, and [Phe^{9,11}]gA channels (top to bottom, respectively). (B) Lifetime distributions, plotted as normalized survivor histograms for gA channels, [Phe^{13,15}]gA channels, and [Phe^{9,11}]gA channels (top to bottom, respectively). The solid curve denotes the normalized survivor distribution, and the interrupted curve denotes the fit of a single-exponential distribution to the results. DPhPC, 1 M NaCl, 200 mV, 25 °C.

Table 1. Single-Channel Properties of Trp → Phe-Substituted gA Analogues[a]

	$g \pm$ SD (pS)[b]		τ (ms)[f]
native gA	15.0 ± 0.2[c]	600 ± 50[c]	840[d]
[Phe^{9}]gA	6.0 ± 0.1[d]		1000[d]
[Phe^{11}]gA	8.7 ± 0.3[d]		2300[d]
[Phe^{13}]gA	11.2 ± 0.2[d]		800[d]
[Phe^{15}]gA	10.9 ± 0.2[d]		800[d]
[Phe^{9,11}] gA	3.9 ± 0.1[c]	1850 ± 100[c]	
[Phe^{13,15}]gA	7.9 ± 0.2[c]	500 ± 50[c]	
[Phe^{9,15}]gA	4.1 ± 0.1[d]		750[d]
[Phe^{9,11,13}]gA	2.1 ± 0.1[d]		2300[d]
[Phe^{9,13,15}]gA	3.0 ± 0.5[d]		5[d]
[Phe^{11,13,15}]gA	3.4 ± 0.1[d]		2100[d]
[Phe^{9,11,13,15}]gA	8.0 ± 0.5[e]		330[e]

[a] DPhPC, 1 M NaCl, 200 mV, 25 °C. [b] Based on two to four individual experiments, with 1000−2000 single-channel current transitions for each channel type. [c] Results from this study. [d] Results from ref 7. [e] Results obtained in 1.0 M CsCl, from ref 4. For comparison, the g for gA is 47 ± 1 ps. The single-channel lifetimes of gA channels in 1.0 M NaCl and CsCl are similar.[53] [f] Based on 500−1000 single-channel events; except where noted, the uncertainty is ∼10%. The single-channel lifetimes in DPhPC/n-decane bilayers have varied over the years, depending in part on the source of the phytanic acid. We therefore list separately the results from this study and those from Becker et al.[7]

the assignments for the C2 and C5 deuterons of the respective major conformations, namely, the SS channel-forming [Phe^{13,15}]gA and the DS nonchannel [Phe^{9,11}]gA.

Trp Ring Orientations and Dynamics. Because the backbone conformation may change in response to the mutation

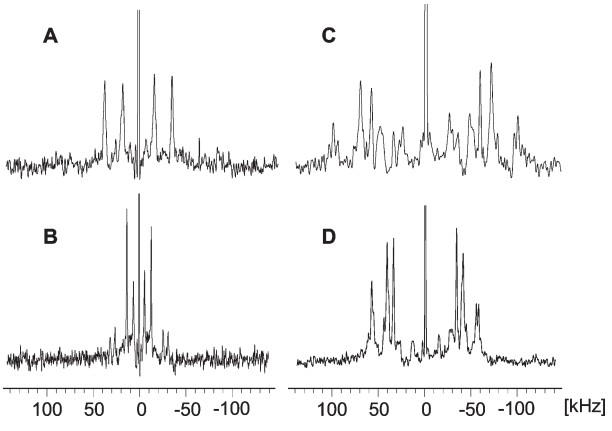

Figure 5. ^{2}H NMR spectra of doubly substituted Trp → Phe gA analogues in oriented DMPC multilayers. (A and B) [Phe^{13,15}]gA with β values of 0° and 90°, respectively. (C and D) [Phe^{9,11}]gA with β values of 0° and 90°, respectively. The temperature was 50 °C.

(Figure 2), it is desirable to examine the Trp side chain orientations without reference to the backbone (i.e., without using χ_1 and χ_2). Moreover, even if the fold of the major conformer is preserved (Figure 2B,D), the detailed backbone geometry may undergo small adjustments. It is therefore useful to describe the indole ring orientations using rotation angles ρ_1 and ρ_2 about axes normal to the ring bridge (Figure 1). As a check on the ring dynamics, we searched the lowest rmsd and the variation of the best-fit values for the ρ_1 and ρ_2 angles as functions of the "apparent" QCC$_{eff}$ (S_{zz} × QCC) value from 120 to 190 kHz for each of the Trp indole rings.[25] These results are summarized in Figure 6, for which the ρ_1 and ρ_2 angles were allowed to vary independently, with neither ρ_1 nor ρ_2 held fixed in any of the

calculations. Although only two data points (C2 and C5) were available for each ring, it is possible to exclude values of QCC_{eff} below ~135 kHz (Figure 6). Values in the range of 135−180 kHz represent a principal ring order parameter S_{zz} between 0.75 and 1.0, although S_{zz} should not exceed the value of ~0.92 established for the gA backbone.[25,31] We conclude that the values of S_{zz} for the indole side chains of the remaining Trps in the major backbone conformers of [$Phe^{13,15}$]gA and [$Phe^{9,11}$]gA fall within a range of approximately 0.75−0.9.

For [$Phe^{13,15}$]gA, which largely retains the SS channel conformation (Figure 2), the ring orientation angle ρ_1 is not very sensitive to S_{zz} (Figure 6A,B). For an S_{zz} assigned anywhere between 0.7 and 0.9 (QCC_{eff} from 130 to 160 kHz), ρ_1 is ~36° for Trp^9 and ~42° for Trp^{11} in [$Phe^{13,15}$]gA. These results should be compared to the similar respective ρ_1 values of ~37° and 46°, respectively, in native gA.[32] Also for the Trps in [$Phe^{9,11}$]gA, regardless of the DS conformation(s) now being dominant (Figure 2), the indole ring orientations remain similar to those in gA.[25] The ρ_1 values for Trp^{13} and Trp^{15} nevertheless become somewhat more sensitive to the choice of S_{zz} (Figure 6C,D). With only two data points, C2 and C5, for each ring, it is not feasible to unambiguously determine S_{zz}, so one is left with a range of 50−55° for ρ_1 for each Trp in [$Phe^{9,11}$]gA.

The values of ρ_2 for Trps in both [$Phe^{9,11}$]gA and [$Phe^{13,15}$]gA show similar behavior and a rather steep dependence upon the exact value of QCC_{eff} [S_{zz} (Figure 6)]. For [$Phe^{13,15}$]gA (Figure 6A,B), ρ_2 varies from ~15° to ~30° over the QCC_{eff} range of 140−170 kHz. For [$Phe^{9,11}$]gA, the dependence of ρ_2 on QCC_{eff} is steeper, varying from ~0° to ~35° over the QCC_{eff} range of 140−170 kHz (Figure 6C,D). Again with only two data points for each Trp ring, we are not able to define exact values for S_{zz} or ρ_2. Nevertheless, for similar ranges of S_{zz}, the trends for ρ_2 as well as ρ_1 correlate with previous findings for the parent gA dimer.[25]

Table 2. ^{2}H Quadrupolar Splittings and Assignments for Trp Rings in Phe-Substituted Gramicidin A Analogues, Oriented at $\beta = 0°$ in DMPC

sequence position	ring position	$\Delta\nu_q$ for [$Phe^{9,11}$]gA (kHz)	$\Delta\nu_q$ for [$Phe^{13,15}$]gA (kHz)	$\Delta\nu_q$ for gA[a] (kHz)
9	2		33	43
11	2		71	96
13	2	124		106
15	2	150		125
9	5		142	151
11	5		170	188
13	5	211		205
15	5	211		205

[a] Data from ref 25.

Heterodimer Formation (test for structural equivalence). Because the doubly Trp → Phe-substituted gA analogues display both SS and DS conformers (Figure 2), we used a heterodimer formation assay,[39] based on channel formation with native SS gA subunits, to establish the conformational identities of the conducting channels formed by the Trp → Phe-substituted gA analogues.[41] In these experiments, native gA subunits are added

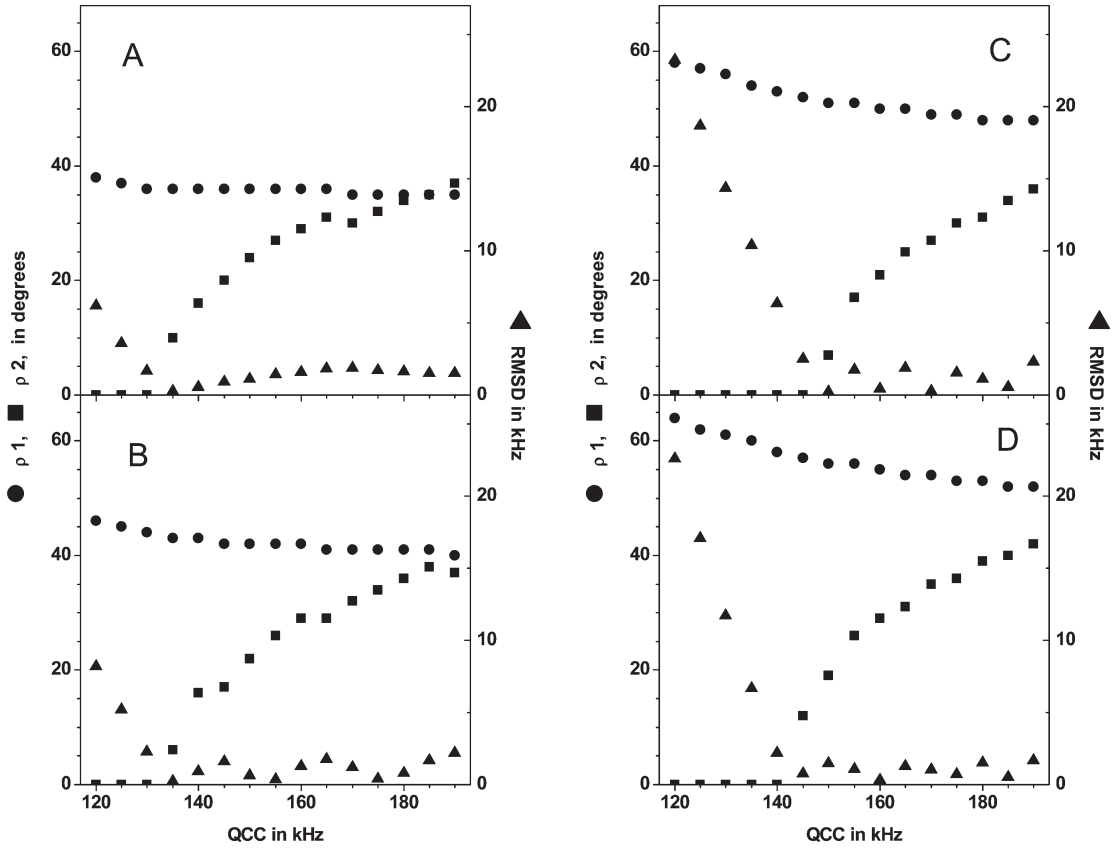

Figure 6. Variation of the best-fit ρ_1 (●), ρ_2 (■), and corresponding rmsd (▲), as functions of apparent QCC for the indole rings of (A) Trp^9 in [$Phe^{13,15}$]gA, (B) Trp^{11} in [$Phe^{13,15}$]gA, (C) Trp^{13} in [$Phe^{9,11}$]gA, and (D) Trp^{15} in [$Phe^{9,11}$]gA.

dx.doi.org/10.1021/bi200136e |*Biochemistry* 2011, 50, 4855–4866

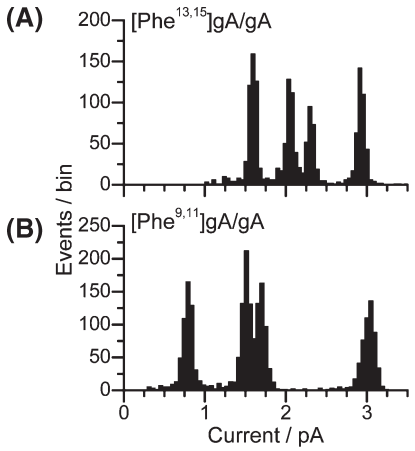

Figure 7. Heterodimer formation experiment with [Phe^{9,11}]gA and native gA, or [Phe^{13,15}]gA, and native gA, added to both sides of a bilayer. (A) Single-channel current transition amplitude histogram with [Phe^{13,15}]gA and native gA. In addition to the two peaks representing the two homodimeric [Phe^{13,15}]gA/[Phe^{13,15}]gA and gA/gA channels, there are two new peaks with intermediate current transition amplitudes, which represent the gA/[Phe^{13,15}]gA and [Phe^{13,15}]gA/gA heterodimeric channels. The orientation of the two peaks, relative to the applied potential, is identified in Figure 8. (The current transition amplitude histograms are based on the cumulative results of individual experiments each obtained using 3−10 different small membranes isolated from the large bilayer using the bilayer punch. The individual histograms obtained from each small membrane displayed a distribution similar to that of the cumulative histograms.) The relative heterodimer appearance rate (eq 1) is 0.73; on the basis of the lifetime distributions (not shown), the relative heterodimer lifetime (eq 2) is 1.03. (B) Single-channel current transition amplitude histogram with [Phe^{9,11}]gA, and native gA. In addition to the two peaks representing the two homodimeric [Phe^{9,11}]gA/[Phe^{9,11}]gA and gA/gA channels, there are two new peaks with intermediate current transition amplitudes, which represent the gA/[Phe^{9,11}]gA and [Phe^{9,11}]gA/gA heterodimeric channels. The orientation of the two peaks, relative to the applied potential, is shown in Figure 8. The relative heterodimer appearance rate (eq 1) is 1.02; on the basis of the lifetime distributions (not shown), the relative heterodimer lifetime (eq 2) is 0.96. DPhPC, 1 M NaCl, 200 mV, 25 °C.

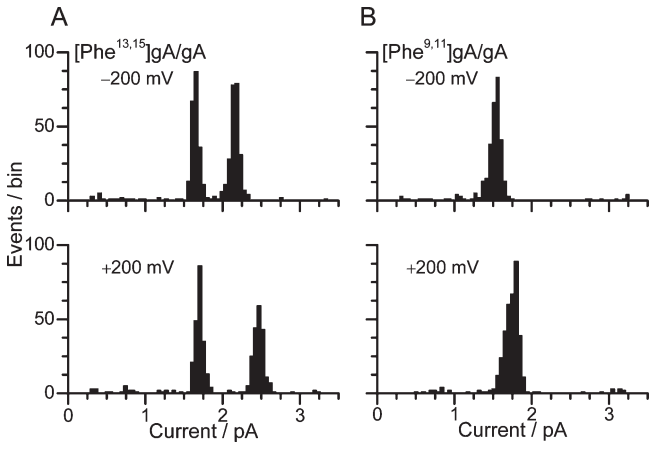

Figure 8. Orientation of the heterodimeric channels underlying the two heterodimer peaks in the current transition amplitude histograms in Figure 7. (A) Results for the [Phe^{13,15}]gA/gA heterodimer, where [Phe^{13,15}]gA is added only to the *cis* compartment (the electrical reference) and the native gA is added only to the *trans* compartment. [Phe^{13,15}]gA is able to cross the bilayer and form single-stranded cation-conducting channels, whereas gA is not, which is evident from the presence of a peak representing the symmetric [Phe^{13,15}]gA homodimeric channels (at ∼1.7 pA) with no corresponding peak representing the symmetric gA homodimeric channels. In the recordings at −200 mV (when the current is toward the gA-containing chamber), the heterodimeric peak is at ∼2.2 pA; in the recordings at 200 mV (when the current is from the gA-containing chamber), the heterodimeric peak is at ∼2.4 pA. (B) Results for the [Phe^{9,11}]gA/gA heterodimer, where [Phe^{9,11}]gA is added only to the *cis* compartment (the electrical reference) and the native gA is added only to the *trans* chamber. In this case, we observe neither of the symmetric, homodimeric channel types. In the recordings at −200 mV (when the current is toward the gA-containing chamber), the most prominent heterodimeric peak is the peak at ∼1.6 pA; in the recordings at 200 mV (when the current is from the gA-containing chamber), the most prominent heterodimeric peak is the peak at ∼1.8 pA.

together with either [Phe^{9,11}]gA or [Phe^{13,15}]gA subunits to both sides of the lipid bilayer. In such experiments, we observe four channel types (Figure 7), the native gA and mutant [Phe^{13,15}]gA or [Phe^{13,15}]gA homodimeric channels, as well as two new channel types with properties that are intermediate between those of the symmetric, homodimeric channels. These new channels are heterodimeric (hybrid) channels formed by one gA and one [Phe^{9,11}]gA or [Phe^{13,15}]gA subunit. The heterodimers can occur in two orientations with respect to the applied potential, gA→[Phe^{x,y}]gA and [Phe^{x,y}]gA→gA, where x and y denote the positions of the Trp → Phe substitutions, depending on whether the current moves from the gA subunit to the [Phe^{x,y}]gA subunit, or vice versa. The heterodimeric channels therefore often exhibit a split peak in a current transition amplitude histogram,[4,42,43] as is the case here. That the hybrid channel conductance is orientation-dependent shows that cations experience an asymmetric barrier when traversing the transmembrane channel. The conductances of the heterodimeric channels, relative to the homodimeric parent channels, can be understood using a simple model in which the Trp → Phe substitution alters primarily the height of the central barrier that has to be traversed by the permeating ions and each subunit's contribution to the change in central barrier is independent of the identity of the other subunit. In this case, one would expect that the geometric mean of the conductances of the heterodimeric channels, $(g_{AB}g_{BA})^{1/2}$, should be equal to the geometric mean of the conductances of the homodimeric channels, $(g_{AA}g_{BB})^{1/2}$, where g_{XY} corresponds to the conductance of channels with that subunit composition (and A denoting gA and B the Trp → Phe-substituted analogue). That is the case for the [Phe^{9,11}]gA/gA heterodimers [$(g_{AB}g_{BA})^{1/2}/(g_{AA}g_{BB})^{1/2} = 1.04 \pm 0.01$ (mean ± SD)] and the [Phe^{13,15}]gA/gA heterodimers [$(g_{AB}g_{BA})^{1/2}/(g_{AA}g_{BB})^{1/2} = 1.02 \pm 0.02$].

The relative appearance rates of homodimer and heterodimer events in the same lipid bilayer membrane serve as a sensitive test of subunit structural equivalence.[39] The reason is that mutually compatible SS partner subunits that display the same backbone fold will form dimers at relative frequencies of appearance that are statistically predictable. (If the subunit fold in the heterodimers differed from that in the homodimers, there would be an energetic penalty for forming heterodimeric channels relative to the homodimeric parent channels.) In the experiments with the doubly substituted Trp → Phe analogues, the observed numbers of heterodimeric channels, relative to the symmetric homodimeric channels, conform to the pattern observed earlier for independent subunit association without an energy barrier for

Table 3. Single-Channel Conductances and Lifetimes of Heterodimeric Channels Formed between [Phe^{9,11}]gA or [Phe^{13,15}]gA and gA

	$g \pm$ SD[a] (pS)	τ[a] (ms)
gA → gA	15.0 ± 0.3	580
gA → [Phe^{9,11}]gA	8.4 ± 0.1	1000
[Phe^{9,11}]gA → gA	7.5 ± 0.2	920
[Phe^{9,11}]gA → [Phe^{9,11}]gA	3.9 ± 0.1	1850
gA → gA	14.7 ± 0.2	640
gA → [Phe^{13,15}]gA	11.5 ± 0.2	560
[Phe^{13,15}]gA → gA	10.2 ± 0.2	610
[Phe^{13,15}]gA → [Phe^{13,15}]gA	7.9 ± 0.2	500

[a] Results from two or three independent experiments conducted with symmetric addition of gA and the Trp → Phe-substituted gA analogue to both sides of the membrane (cf., Figure 7), each with 3−10 small membranes isolated using the bilayer punch. The orientation of the heterodimeric channels was determined from the results in Figure 8. The uncertainty in the single-channel lifetimes is ∼10%.

refolding,[39,41] namely the relative number of heterodimeric channels (Rn_H), given by

$$Rn_H = \sqrt{\frac{n_{AB}n_{BA}}{n_{AA}n_{BB}}} \quad (1)$$

where n_{XY} corresponds to the number of appearances of channels with that subunit composition and is close to 1.0. (Because all the n_{XY} values are determined in the same experiment, in the same membrane over the same time interval, Rn_H is equal to the relative appearance rate for the hybrid channels.[39,41]) For the [Phe^{9,11}]gA/gA combination, $Rn_H \approx 1.02$; for the [Phe^{13,15}]gA/gA combination, $Rn_H \approx 0.73$. In either case, there are few if any subunit-specific interactions (cf., ref 39), such that we conclude that there is structural equivalence among the channel-forming subunits.

The respective heterodimer orientations that underlie the two hybrid channel peaks in the current transition amplitude histograms can be established in experiments in which one analogue is added to only one side of a bilayer and the other analogue to the other side.[4] In such experiments, we observed shifts in the distribution of transitions in the heterodimer peaks, reflecting the fact that the magnitude of the current through the heterodimeric channels varies with the polarity of the applied potential (Figure 8). In the [Phe^{13,15}]gA/gA experiments, we observed two peaks, one peak (at ∼1.7 pA) representing symmetric [Phe^{13,15}]gA channels and another peak representing the [Phe^{13,15}]gA/gA heterodimers. At −200 mV (when the current flow is from [Phe^{13,15}]gA to gA), the heterodimer peak is at ∼2.1 pA; at 200 mV (when the current flow is from gA to [Phe^{13,15}]gA), the heterodimer peak is at ∼2.4 pA. That is, the current flow in the gA → [Phe^{13,15}]gA direction is greater than the current flow in the reverse direction (Figure 8A). In the [Phe^{9,11}]gA/gA experiments, we observed only one peak, representing the [Phe^{9,11}]gA/gA heterodimers. At −200 mV (when the current flow is from [Phe^{9,11}]gA to gA), the heterodimer peak is at ∼1.6 pA; at 200 mV (when the current flow is from gA to [Phe^{9,11}]gA), the heterodimer peak is at ∼1.8 pA. Again, the current flow in the gA → gA[Phe^{9,11}] direction is greater than the current flow in the [Phe^{9,11}]gA → gA direction (Figure 8B).

With the respective channel orientations known (Figure 8), it becomes possible to assign the single-channel current magnitude and lifetime for each of the heterodimeric channels in both orientations. Not only the single-channel current transitions but also the single-channel lifetimes vary as a function of the orientation of the heterodimeric channels with respect to the applied potential (Table 3). Though the difference is small compared to the experiment-to-experiment variation, the relative difference determined in individual experiments, $(\tau_{AB} - \tau_{BA})/(\tau_{AA}\tau_{BB})^{1/2}$, where τ_{XY} corresponds to the lifetime of the channels with the XY subunit composition, is different from zero: 0.14 ± 0.05 (mean ± range) for the [Phe^{9,11}]gA/gA heterodimer and 0.10 ± 0.02 for the [Phe^{13,15}]gA/gA heterodimer. As was the case for the channel appearances, the single-channel lifetimes of the heterodimeric channels, relative to those of the symmetric homodimeric channels, conform to the statistically predictable pattern observed previously,[39,41] namely that the relative heterodimer lifetime ($R\tau_H$), given by

$$R\tau_H = \frac{\sqrt{\tau_{AB}\tau_{BA}}}{\sqrt{\tau_{AA}\tau_{BB}}} \quad (2)$$

is close to 1.0. For the [Phe^{9,11}]gA/gA combination, $R\tau_H \approx 1.03$; for the [Phe^{13,15}]gA/gA combination, $R\tau_H \approx 0.96$. In either case, there is little if any subunit-specific strain at the subunit interface (cf., ref 39).

DISCUSSION

We report on the use of a method for deuterium labeling of Trp indole rings in already existing peptides to explore the consequences of double Trp → Phe mutations in gA channels. In separate experiments, the inner pair and then the outer pair of anchoring Trp residues were "mutated" to Phe, by means of chemical synthesis. By using the method for deuterium labeling of already existing peptides, we were able to introduce deuterium onto the peptide-incorporated indole rings selectively, at positions C2 and C5 of each tryptophan, for use in solid-state ^{2}H NMR experiments. The Trp → Phe substitutions alter the gA analogues' conformational preference. Using a backbone-independent analysis,[25] the assigned spectra from two different labeled Trps in each doubly Phe-substituted gA analogue were used to examine the changes in average indole ring orientations induced by the Phe substitutions. In turn, we will discuss the backbone folding preferences, average indole ring orientations, and conducting channel structure and function, as revealed by the single-channel conductances and lifetimes.

Folding Preference of Doubly Phe-Substituted gA Analogues. The conformational consequences of the double Trp → Phe substitutions were examined using CD spectroscopy and SE chromatography. Generally, it is known that there are two general classes of folding patterns for gA, resulting in two different types of conformations. One conformational class is the (right-handed) head-to-head, SS $\beta^{6.3}$-helix, which functions as a cation-conducting channel.[45,46] The other conformational class is a family of DS intertwined double helices.[47−50]

The CD spectra of the doubly Phe-substituted gramicidin analogues in DMPC vesicles are dominated by these two different patterns of folding. The spectrum of [Phe^{13,15}]gA is similar to that of native gA in DMPC bilayers (Figure 2), indicating that [Phe^{13,15}]gA adopts predominantly the SS $\beta^{6.3}$-helical channel conformation. The spectrum of [Phe^{9,11}]gA is quite different, suggesting that the analogue adopts predominantly a DS (nonconducting) conformation. The CD spectra of the doubly Phe-substituted gramicidin analogues thus suggest different effects on the peptide secondary

structure preference in lipid bilayers based upon the different positions of Trp indole side chains.

The size-exclusion chromatography (SEC) results agree with the conclusions from the CD spectra. For [Phe^{13,15}]gA, ~75% of this analogue elutes from the SEC column as monomers. The most likely interpretation of the SEC elution profile is that 75% of [Phe^{13,15}]gA remains in the SS $\beta^{6.3}$-helical channel structure in lipid bilayers. The SS conformation of [Phe^{13,15}]gA (but not of [Phe^{9,11}]gA) therefore is expected to dominate the NMR spectra. In contrast, the SEC elution profile of [Phe^{9,11}]gA in DMPC shows that the majority of this analogue elutes as DS dimers, suggesting that this peptide prefers a DS conformation rather than the SS channel structure in DMPC. The SEC results thus support the conclusion from the CD analysis that substitution of the inner, more buried, Trps at positions 9 and 11 significantly shifts the gramicidin A structure away from the SS channel conformation toward the DS dimer conformation. Qualitatively similar results were reported by Salom et al.[20] These changes in conformational preference reflect primarily the removal of the indole NH group, not the introduction of the Phe, as a similar shift in conformational preference was observed when Trp was replaced with *N*-methyl-Trp.[17]

In general, the energetic cost of burying the four Trps within the lipid bilayer makes it unfavorable for native gA to remain folded in the DS nonconducting conformation.[3] Phe, like Trp, is an aromatic amino acid but is less polar and lacks hydrogen bonding ability, whereas Trp is amphipathic and able to be a hydrogen bond donor by means of the indole NH group. Trp furthermore has a dipole moment of ≈2 D along the C5 → N1 axis.[13] The observed conformational shift thus may be due to these differences between the Trp and Phe side chain characteristics, with the hydrogen bond formation likely to be dominant.[17] Because of the loss of hydrogen bonding ability, the Phe ring can be buried more deeply than the Trp ring, which becomes important because the DS conformations will bury side chains 9 and 11 essentially near the bilayer center. It therefore should not be surprising that Trp → Phe substitutions at positions 9 and 11 (but less so at positions 13 and 15) allow a conformational shift from SS toward DS gramicidin conformers.

Effect of Double Phe Substitution on the Remaining Trp Indole Ring Orientations. For the analysis of Trp indole ring orientations, two labels (C2 and C5) are available for each Trp ring. The assignments of observed quadrupolar splittings to ring positions C2 and C5 are unambiguous, based upon the distinct and strong correlation between the rate of ^{2}H chemical exchange (during sample preparation) and the intensities of the subsequently observed ^{2}H NMR peaks, in the following order: C2 ≫ C5 ≫ other ring positions.[25] The changes in the C2−D and C5−D quadrupolar splitting for each ring indicate that the Trp indole rings in gA did undergo modest changes in their orientations upon replacement of two nearby Trps with Phe. With the ring position (C2 and C5) peak assignments known, we adopted a "minimalist" approach and used the principle of "least change", thereby assigning each set of two quadrupolar splittings (having comparable intensities within the set) to the remaining Trps in the sequence, such that the overall assignments for the set were most similar to the known quadrupolar splitting assignments[25] for the native gA channel.

Comparing the orientations for each indole ring in [Phe^{9,11}]gA and [Phe^{13,15}]gA, one finds that the acceptable ranges of ρ_1 and ρ_2, for example, ρ_1 values of ~36−42° for Trp^9 and Trp^{11}, are similar to those observed for the gA channel itself,[25] suggesting that the orientation of any Trp residue is not much altered by Trp → Phe substitutions at other positions or by the change in backbone conformation. It appears, therefore, that the observed indole ring orientations are probably determined more by the properties of the membrane−water interface than by the backbone conformation. The trends in ρ_2 (Figure 6) are more dependent upon the assumed value of S_{zz}, which is not accurately determined from the available data. The qualitative differences between the inner pair as compared to the outer pair indole ring behavior (Figure 6) are preserved from gA itself.[25]

Single-Channel Properties. In contrast to the NMR experiments, as demonstrated by the heterodimer experiments, the single-channel experiments report exclusively on the properties of the SS conformation, for both [Phe^{13,15}]gA (where it is the major conformer) and [Phe^{9,11}]gA (where it is the minor conformer). To be consistent with the [Phe^{9,11}]gA channels being formed by the minor conformer, we needed to add 10-fold higher concentrations of [Phe^{9,11}]gA than of [Phe^{13,15}]gA or gA to observe equivalent numbers of channel events. The fact that the fold of the channel-forming subunits is similar can be deduced by calculating the energetic cost of forming the heterodimeric channels, relative to the homodimeric channels ($\Delta\Delta G^\circ$), which is estimated as[40,41]

$$\Delta\Delta G^\circ = \Delta G^\circ_H - \frac{\Delta G^\circ_{AA} + \Delta G^\circ_{BB}}{2} = -\frac{k_B T}{2}\ln(Rn_H R\tau_H) \quad (3)$$

where ΔG°_H, ΔG°_{AA}, and ΔG°_{BB} denote the free energy of forming heterodimers and the symmetric homodimers, respectively, k_B is Boltzmann's constant, and T is the temperature in kelvin. Using the values for Rn_H and $R\tau_H$ reported in Figure 7, $\Delta\Delta G^\circ$ is within 1 kJ/mol of zero. We conclude that the conformers of [Phe^{9,11}]gA and [Phe^{13,15}]gA that assemble to form the conducting channels are structurally equivalent to the channels with SS subunits formed by the native gA. In terms of channel function, therefore, the observed differences in the single-channel conductances and lifetimes reflect the consequences of the different Trp indole ring positions within the context of a fixed backbone conformation for these inner and outer sequence isomers.

When the outer Trp^{13} and Trp^{15} are removed, the effects are modest (Table 1): the single-channel conductance is ~50% lower, and the lifetime is reduced by 10−20%. These results are expected because each of the four Trps enhances the flow of cations through native gA channels[7] because of favorable ion−dipole interactions that lower the energy barrier for crossing the channel center,[9,10] and the outer Trps interact favorably with water and/or polar groups at the membrane−water interface and stabilize the SS dimeric transmembrane channel.

The changes in channel properties are more dramatic when the inner Trp^9 and Trp^{11} are removed. The observed increase in the lifetime, together with the decreased conductance, serves to emphasize that the single-channel conductance and lifetime are independent properties, extending previous conclusions.[7,51] The single-channel conductance for [Phe^{9,11}]gA is ~25% of that of native gA channels, thus illustrating the importance of the inner Trp^9 and Trp^{11} residues for the cation conductance. The larger changes in the single-channel conductance, relative to the [Phe^{13,15}]gA channels, reflect in part the fact that the Trp^9 and Trp^{11} side chain dipoles are closer to the channel center. Trp^9 and Trp^{11} therefore would be expected to have stronger effects

on the energy barrier for the movement of ions through the pore, consistent with previous kinetic analyses,[44,52] which showed that Trp^{9} has a strong effect on the rate constant for crossing the central barrier[44] and that replacing all four Trps (in $[Phe^{9,11,13,15}]$gA, also known as gramicidin M) also causes large changes in the rate constant for crossing the central barrier.[52] Trp → Phe substitutions also alter the kinetics of ion entry and exit.[44,52] At the same time, the transmembrane dimers show 3-fold longer lifetimes (Table 1) when Trp^{9} and Trp^{11} are absent. Interestingly, a dramatically short lifetime of 5 ms is observed for the triply substituted $[Phe^{9,13,15}]$gA,[7] namely when only Trp^{11} is present. It is evident that Trp^{11} destabilizes the transmembrane dimer whereas Trp^{13} and Trp^{15} serve to increase the lifetimes of the conducting dimers. Trp^{9} often contributes a mild stabilization, although its detailed influence on the single-channel lifetime depends upon the context in which other tryptophans are present.

The properties of the heterodimeric channels add to this picture. Because each of the analogue subunits combines readily with a native gA SS subunit, with little if any strain at the subunit interface, all of the conducting channels indeed are formed by SS $\beta^{6.3}$-helical subunits.

The heterodimer experiments also provide insight into the conductance changes caused by Trp → Phe substitutions. The geometric mean of the single-channel conductances of the hybrid channels is equal to the geometric mean of the conductances of the symmetric parent channels, with the ratio $[(g_{AB}g_{BA})/(g_{AA}g_{BB})]^{1/2}$ being close to 1 (1.04 for the $[Phe^{9,11}]$gA/gA pair and 1.02 for the $[Phe^{13,15}]$gA/gA pair). This result suggests that the Trp → Phe substitutions in each subunit have independent effects on the energy barrier for crossing the channel center, meaning that the peak height of the energy barrier in the heterodimers is the algebraic mean of the peak height in the homodimers. The situation is more complicated, however, which is evident from the split in the peaks representing the hybrid channels in the current transition amplitude histograms (Figures 7 and 8). This asymmetry shows, as expected, that the energy barrier that the ions have to surmount to move through the channel is asymmetric in the heterodimeric channels. The asymmetry in the peaks representing the heterodimers, defined as $(g_{AB} - g_{BA})/(g_{AA}g_{BB})^{1/2}$, is similar in magnitude (between 0.12 and 0.13) for the $[Phe^{9,11}]$gA/gA and $[Phe^{13,15}]$gA/gA heterodimers even though Trp^{9} and Trp^{11} are closer to the channel center than Trp^{13} and Trp^{15}.

We finally note that we observed only symmetric $[Phe^{13,15}]$gA, not $[Phe^{9,11}]$gA, channels when the gA analogues were added to only one side of the bilayer. (We did not observe symmetric gA channels after asymmetric addition to only one side of the bilayer, consistent with previous observations.[2]) The different behavior of $[Phe^{13,15}]$gA could reflect its conformational preferences. One would expect that the DS conformers could insert and span the bilayer. If the DS conformers are the preferred conformers, then they may not readily dissociate but rather remain as bilayer-spanning entities, which would account for why we did not observe many symmetric SS $[Phe^{9,11}]$gA channels. If, however, the DS conformers are not preferred, they could dissociate following insertion and fold into SS conformers at both interfaces, which would account for the observation of symmetric, SS $[Phe^{13,15}]$gA channels after asymmetric addition of the analogue. Further details of these phenomena are under investigation.

Summary and Conclusions. The average indole ring orientations and overall motion of Trp rings in doubly Phe-substituted gA analogues ($[Phe^{13,15}]$gA and $[Phe^{9,11}]$gA) were defined by experimental ^{2}H NMR spectra. Backbone conformations were monitored by CD spectroscopy and SEC. The results show that the substitution of two Trps in a gramicidin subunit with Phe may alter the backbone conformation of lipid membrane-incorporated gramicidin, depending upon the positions of the substitutions. The $[Phe^{13,15}]$gA analogue adopts predominantly the SS $\beta^{6.3}$-helical channel conformation, whereas the $[Phe^{9,11}]$gA analogue adopts predominantly a DS nonconducting conformation. The Phe substitutions alter only slightly the average orientations of the remaining tryptophans, based on only modest changes in the observed indole ring ^{2}H quadrupolar splittings in response to the Phe substitutions. For both analogues, the cation-conducting channels are single-stranded $\beta^{6.3}$-helical dimers, and the single-channel results reveal that the dipoles of Trp^{9} and Trp^{11} are relatively more important for the cation conductance than are the dipoles of Trp^{13} and Trp^{15}.

AUTHOR INFORMATION

Corresponding Author

*R.E.K.: telephone, (479) 575-4976; fax, (479) 575-4049; e-mail, rk2@uark.edu. O.S.A.: telephone, (212) 746-6350; fax, (212) 746-8678; e-mail, sparre@med.cornell.edu.

Funding Sources

This work was supported in part by National Institutes of Health Grants GM70971, GM21342, RR15569, and RR31154 and by the Arkansas Biosciences Institute.

ABBREVIATIONS

CD, circular dichroism; DMPC, 1,2-dimyristoylphosphatidylcholine; DPhPC, 1,2-diphytanoylphosphatidylcholine; DMF, dimethylformamide; DS, double-stranded; gA, gramicidin A; MS, mass spectrometry; NMR, nuclear magnetic resonance; QCC, quadrupolar coupling constant; SD, standard deviation; SEC, size-exclusion chromatography; SS, single-stranded; TFA, trifluoroacetic acid.

REFERENCES

(1) Ketchem, R. R., Hu, W., and Cross, T. A. (1993) High-resolution of gramicidin A in a lipid bilayer by solid-state NMR. *Science 261*, 1457–1460.

(2) O'Connell, A. M., Koeppe, R. E., II, and Andersen, O. S. (1990) Kinetics of gramicidin channel formation in lipid bilayers: Transmembrane monomer association. *Science 250*, 1256–1259.

(3) Durkin, J. T., Providence, L. L., Koeppe, R. E., II, and Andersen, O. S. (1992) Formation of non-$\beta^{6.3}$-helical gramicidin channels between sequence-substituted gramicidin analogues. *Biophys. J. 62*, 145–159.

(4) Fonseca, V., Daumas, P., Ranjalahy Rasoloarijao, L., Heitz, F., Lazaro, R., Trudelle, Y., and Andersen, O. S. (1992) Gramicidin channels that have no tryptophan residues. *Biochemistry 31*, 5340–5350.

(5) Hu, W., Lee, K. C., and Cross, T. A. (1993) Tryptophans in membrane proteins: Indole ring orientations and functional implications in the gramicidin channel. *Biochemistry 32*, 7035–7047.

(6) Arumugam, S., Pascal, S., North, C. L., Hu, W., Lee, K. C., Cotten, M., Ketchem, R. R., Xu, M., Brenneman, M., Kovacs, F., Tian, F., Wang, A., Huo, S., and Cross, T. A. (1996) Conformational trapping in a membrane environment: A regulatory mechanism for protein activity? *Proc. Natl. Acad. Sci. U.S.A. 93*, 5872–5876.

(7) Becker, M. D., Greathouse, D. V., Koeppe, R. E., and Andersen, O. S. (1991) Amino acid sequence modulation of gramicidin channel function: Effects of tryptophan-to-phenylalanine substitutions on the single-channel conductance and duration. *Biochemistry 30*, 8830–8839.

(8) Hu, W., and Cross, T. A. (1995) Tryptophan hydrogen bonding and electric dipole moments: Functional roles in the gramicidin channel and implications for membrane proteins. *Biochemistry 34*, 14147–14155.

(9) Andersen, O. S., Greathouse, D. V., Providence, L. L., Becker, M. D., and Koeppe, R. E., II (1998) Importance of tryptophan dipoles for protein function: 5-Fluorination of tryptophans in gramicidin A channels. *J. Am. Chem. Soc. 120*, 5142–5146.

(10) Dorigo, A. E., Anderson, D. G., and Busath, D. D. (1999) Noncontact dipole effects on channel permeation. II. Trp conformations and dipole potentials in gramicidin A. *Biophys. J. 76*, 1897–1908.

(11) Cotten, M., Tian, C., Busath, D. D., Shirts, R. B., and Cross, T. A. (1999) Modulating dipoles for structure-function correlations in the gramicidin A channel. *Biochemistry 38*, 9185–9197.

(12) Cole, C. D., Frost, A. S., Thompson, N., Cotten, M., Cross, T. A., and Busath, D. D. (2002) Noncontact dipole effects on channel permeation. VI. 5F- and 6F-Trp gramicidin channel currents. *Biophys. J. 83*, 1974–1986.

(13) Weiler-Feilchenfeld, H. A., Pullman, A., Berthod, H., and Giessner-Trettre, C. (1970) Experimental and quantum-chemical studies of the dipole moments of quinoline and indole. *J. Mol. Struct. 6*, 297–304.

(14) Bamberg, E., Noda, K., Gross, E., and Läuger, P. (1976) Single-channel parameters of gramicidin A, B, and C. *Biochim. Biophys. Acta 419*, 223–228.

(15) Sawyer, D. B., Williams, L. P., Whaley, W. L., Koeppe, R. E., II, and Andersen, O. S. (1990) Gramicidins A, B, and C form structurally equivalent ion channels. *Biophys. J. 58*, 1207–1212.

(16) Heitz, F., Spach, G., and Trudelle, Y. (1982) Single channels of 9,11,13,15-destryptophyl-phenylalanyl-gramicidin A. *Biophys. J. 40*, 87–89.

(17) Sun, H., Greathouse, D. V., Andersen, O. S., and Koeppe, R. E., II (2008) The preference of tryptophan for membrane interfaces: Insights from N-methylation of tryptophans in gramicidin channels. *J. Biol. Chem. 283*, 22233–22243.

(18) Gu, H., Thomas, G., Subotic, A., Liyanage, R., Lay, J., Koeppe, R. E., II, and Greathouse, D. G. (2005) *In situ* deuteration of Trp indole rings in peptides. *Biophys. J. 88*, 141a (abstract).

(19) Heitz, F., Gavach, C., Spach, G., and Trudelle, Y. (1986) Analysis of the ion transfer through the channel of 9,11,13,15-phenylalanylgramicidin A. *Biophys. Chem. 24*, 143–148.

(20) Salom, D., Pérez-Payá, E., Pascal, J., and Abad, C. (1998) Environment- and sequence-dependent modulation of the double-stranded to single-stranded conformational transition of gramicidin A in membranes. *Biochemistry 37*, 14279–14291.

(21) Greathouse, D. V., Koeppe, R. E., II, Providence, L. L., Shobana, S., and Andersen, O. S. (1999) Design and characterization of gramicidin channels. *Methods Enzymol. 294*, 525–550.

(22) Gu, H. (2008) Application of tryptophan derivatives for studies of membrane-spanning peptides, Ph.D. Thesis, University of Arkansas, Fayetteville, AR.

(23) Van der Wel, P. C. A., Strandberg, E., Killian, J. A., and Koeppe, R. E., II (2002) Geometry and intrinsic tilt of a tryptophan-anchored transmembrane α-helix determined by ^{2}H NMR. *Biophys. J. 83*, 1479–1488.

(24) Dvinskikh, S. V., Castro, V., and Sandstrom, D. (2005) Probing segmental order in lipid bilayers at variable hydration levels by amplitude- and phase-modulated cross-polarization NMR. *Phys. Chem. 7*, 3255–3257.

(25) Koeppe, R. E., II, Sun, H., van der Wel, P. C. A., Scherer, E. M., Pulay, P., and Greathouse, D. V. (2003) Combined Experimental/Theoretical Refinement of Indole Ring Geometry using Deuterium Magnetic Resonance and *ab initio* Calculations. *J. Am. Chem. Soc. 125*, 12268–12276.

(26) van der Wel, P. C. A., Reed, N. D., Greathouse, D. V., and Koeppe, R. E., II (2007) Orientation and motion of tryptophan interfacial anchors in membrane-spanning peptides. *Biochemistry 46*, 7514–7524.

(27) Koeppe, R. E., II, Killian, J. A., and Greathouse, D. V. (1994) Orientations of the tryptophan 9 and 11 side chains of the gramicidin channel based on deuterium NMR spectroscopy. *Biophys. J. 66*, 14–24.

(28) McKeone, B. J., Pownall, H. J., and Massey, J. B. (1986) Ether phosphatidylcholines: Comparison of miscibility with ester phosphatidylcholines and sphingomyelin, vesicle fusion, and association with apolipoprotein A-1. *Biochemistry 25*, 7711–7716.

(29) Davis, J. H., Jeffrey, K. R., Valic, M. I., Bloom, M., and Higgs, T. P. (1976) Quadrupolar echo deuteron magnetic resonance spectroscopy in ordered hydrocarbon chains. *Chem. Phys. Lett. 42*, 390–394.

(30) Gall, C. M., DiVerdi, J. A., and Opella, S. J. (1981) Phenylalanine ring dynamics by solid-state ^{2}H NMR. *J. Am. Chem. Soc. 103*, 5039–5043.

(31) Killian, J. A., Taylor, M. J., and Koeppe, R. E., II (1992) Orientation of the valine-1 side chain of the gramicidin transmembrane channel and implications for channel functioning. A ^{2}H NMR study. *Biochemistry 31*, 11283–11290.

(32) Pulay, P., Scherer, E. M., van der Wel, P. C. A., and Koeppe, R. E., II (2005) Importance of Tensor Asymmetry for the Analysis of ^{2}H NMR Spectra from Deuterated Aromatic Rings. *J. Am. Chem. Soc. 127*, 17488–17493.

(33) Greathouse, D. V., Hinton, J. F., Kim, K. S., and Koeppe, R. E., II (1994) Gramicidin A/short-chain phospholipid dispersions: Chain length dependence of gramicidin conformation and lipid organization. *Biochemistry 33*, 4291–4299.

(34) Turner, G. L., Hinton, J. F., Koeppe, R. E., II, Parli, J. A., and Millett, F. S. (1983) Difference in association of thallium(I) with gramicidin A and gramicidin B in trifluoroethanol determined by thallium-205 NMR. *Biochim. Biophys. Acta 756*, 133–137.

(35) Bañó, M. C., Braco, L., and Abad, C. (1988) New high-performance liquid chromatography-based methodology for monitoring the conformational transitions of self-associating hydrophobic peptides, incorporated into liposomes. *J. Chromatogr. 458*, 105–116.

(36) Andersen, O. S. (1983) Ion movement through gramicidin A channels. Single-channel measurements at very high potentials. *Biophys. J. 41*, 119–133.

(37) Sawyer, D. B., Koeppe, R. E., II, and Andersen, O. S. (1990) Gramicidin single-channel properties show no solvent-history dependence. *Biophys. J. 57*, 515–523.

(38) Sawyer, D. B., Koeppe, R. E., II, and Andersen, O. S. (1989) Induction of conductance heterogeneity in gramicidin channels. *Biochemistry 28*, 6571–6583.

(39) Durkin, J. T., Koeppe, R. E., II, and Andersen, O. S. (1990) Energetics of gramicidin hybrid channel formation as a test for structural equivalence. Side-chain substitutions in the native sequence. *J. Mol. Biol. 211*, 221–234.

(40) Andersen, O. S., Bruno, M. J., Sun, H., and Koeppe, R. E., II (2007) Single-molecule methods for monitoring changes in bilayer elastic properties. *Methods Mol. Biol. 400*, 541–568.

(41) Durkin, J. T., Providence, L. L., Koeppe, R. E., II, and Andersen, O. S. (1993) Energetics of heterodimer formation among gramicidin analogues with an NH_2-terminal addition or deletion: Consequences of missing a residue at the join in the channel. *J. Mol. Biol. 231*, 1102–1121.

(42) Mazet, J. L., Andersen, O. S., and Koeppe, R. E., II (1984) Single-channel studies on linear gramicidins with altered amino acid sequences. A comparison of phenylalanine, tryptophan, and tyrosine substitutions at positions 1 and 11. *Biophys. J. 45*, 263–276.

(43) Russell, E. W. B., Weiss, L. B., Navetta, F. I., Koeppe, R. E., II, and Andersen, O. S. (1986) Single-channel studies on linear gramicidins with altered amino acid side chains. Effects of altering the polarity of the side chain at position 1 in gramicidin A. *Biophys. J. 49*, 673–686.

(44) Becker, M. D., Koeppe, R. E., II, and Andersen, O. S. (1992) Amino acid substitutions and ion channel function. Model-dependent conclusions. *Biophys. J. 62*, 25–27.

(45) Urry, D. W. (1971) The gramicidin A transmembrane channel: A proposed π(L,D) helix. *Proc. Natl. Acad. Sci. U.S.A. 68*, 672–676.

(46) Andersen, O. S., Apell, H.-J., Bamberg, E., Busath, D. D., Koeppe, R. E., II, Sigworth, F. J., Szabo, G., Urry, D. W., and Woolley, A. (1999) Gramicidin channel controversy: The structure in a lipid environment. *Nat. Struct. Biol. 6*, 609.

(47) Veatch, W. R., Fossel, E. T., and Blout, E. R. (1974) Conformation of gramicidin A. *Biochemistry 13*, 5249–5256.

(48) Langs, D. A. (1988) Three-dimensional structure at 0.86 Å of the uncomplexed form of the transmembrane ion channel peptide gramicidin A. *Science 241*, 188–191.

(49) Bouchard, M., Benjamin, D. R., Tito, P., Robinson, C. V., and Dobson, C. M. (2000) Solvent effects on the conformation of the transmembrane peptide gramicidin A: Insights from electrospray ionization mass spectrometry. *Biophys. J. 78*, 1010–1017.

(50) Burkhart, B. M., Li, N., Langs, D. A., Pangborn, W. A., and Duax, W. L. (1998) The conducting form of gramicidin A is a right-handed double-stranded double helix. *Proc. Natl. Acad. Sci. U.S.A. 95*, 12950–12955.

(51) Andersen, O. S., Providence, L. L., Mattice, G. L., and Koeppe, R. E., II (1997) Ion channels with L- and D-amino acids. *Chemtracts: Biochem. Mol. Biol. 10*, 175–188.

(52) Durrant, J. D., Caywood, D., and Busath, D. D. (2006) Tryptophan contributions to the empirical free-energy profile in gramicidin A/M heterodimer channels. *Biophys. J. 91*, 3230–3241.

(53) Mattice, G. L., Koeppe, R. E., II, Providence, L. L., and Andersen, O. S. (1995) Stabilizing effect of D-alanine-2 in gramicidin channels. *Biochemistry 34*, 6827–6837.